PHYSICAL REVIEW C **76**, 044005 (2007)

Helicity dependence and contribution to the Gerasimov-Drell-Hearn sum rule of the $\vec{\gamma}\vec{d} \to \pi NN$ reaction channels in the energy region from threshold up to the $\Delta(1232)$ resonance

E. M. Darwish,[1,*] C. Fernández-Ramírez,[2,3,†] E. Moya de Guerra,[2,4] and J. M. Udías[4]
[1]*Physics Department, Faculty of Science, Sohag University, Sohag 82524, Egypt*
[2]*Instituto de Estructura de la Materia, CSIC, Serrano 123, E-28006 Madrid, Spain*
[3]*Departamento de Física Atómica, Molecular y Nuclear, Universidad de Sevilla, Apdo. 1065, E-41080 Sevilla, Spain*
[4]*Grupo de Física Nuclear; Departamento de Física Atómica, Molecular y Nuclear, Facultad de Ciencias Físicas, Universidad Complutense de Madrid, Avda. Complutense s/n, E-28040 Madrid, Spain*
(Received 18 January 2007; published 15 October 2007)

The helicity dependence of the $\vec{\gamma}\vec{d} \to \pi^- pp$, $\vec{\gamma}\vec{d} \to \pi^+ nn$, and $\vec{\gamma}\vec{d} \to \pi^0 np$ reaction channels is studied for incident photon energies from threshold up to the $\Delta(1232)$ resonance with inclusion of leading πNN effects. The doubly polarized total and differential cross sections for parallel and antiparallel helicity states are predicted. Then the contribution of various channels to the deuteron spin asymmetry and the double polarization E asymmetry is calculated. In addition, the contribution to the Gerasimov-Drell-Hearn (GDH) integral from separate channels is evaluated by explicit integration up to a photon lab energy of 350 MeV. Sizeable effects from final-state interactions, specially for π^0 production, are found. The sensitivity of the results to the elementary pion photoproduction operator is also investigated. Considerable dependence of the results on the elementary amplitude is found. We expect that these results may be useful to interpret the recent measurements from LEGS@BNL, A2, and GDH@MAMI Collaborations.

DOI: 10.1103/PhysRevC.76.044005 PACS number(s): 13.60.Le, 25.20.Lj, 14.20.−c, 29.27.Hj

I. INTRODUCTION

Recent years have witnessed an increasing interest in theoretical research on quasifree pion production from the deuteron including polarization observables—see recent works in Refs. [1–4] where also references to earlier research can be found. This interest is partly due to the new generation of high-intensity and high duty-cycle electron accelerators, such as MAMI at Mainz and ELSA at Bonn (Germany), JLab at Newport News (USA), and MAX-Lab at Lund (Sweden) as well as laser backscattering facilities such as GRAAL at Grenoble (France) and LEGS at Brookhaven (USA)—for an experimental overview see Refs. [5–8]. With the development of these new facilities, and thanks to the improvement in polarized beam and polarized target techniques, it is now possible to obtain accurate data for meson electromagnetic production, including single and double spin-dependent observables. These measurements allow us to obtain more information on the reaction mechanism than unpolarized measurements do. The latter only provide information on the sum of the absolute squares of the reaction amplitudes.

A series of measurements of double polarization observables in both charged and neutral pion production reactions from the deuteron have been carried out or planned at different laboratories such as LEGS and MAMI.

In particular, the A2 and GDH Collaborations at MAMI have undertaken a joint effort to verify experimentally the Gerasimov-Drell-Hearn (GDH) sum rule [9], measuring the difference between the helicity components in both the total $[\sigma^P - \sigma^A]$ and the differential $[d(\sigma^P - \sigma^A)/d\Omega]$ photoabsorption cross sections, where $\sigma^{P,A}$ stands for the parallel and antiparallel spin orientations of the photon and target deuteron. In these experiments, circularly polarized photons are scattered on longitudinally polarized deuterons to determine the double polarization asymmetry in a large kinematical range [6]. These helicity-dependent cross sections provide valuable information on the nucleon spin structure and allow us to extract information on the neutron. The knowledge of these cross sections is also required to test the validity of the GDH sum rule on the deuteron and the neutron as well as to explore which are the dominant contributions to the GDH integral. These new measurements will make possible to test experimentally the behavior of the GDH integral.

However, to explore the contributions of the resonances, the total photoabsorption cross section does not provide enough information. Fixing degrees of freedom by selection of particular partial reaction channels allows us to obtain more detailed information. This is possible with double polarization observables of the differential cross section. The present focus of the LEGS Collaboration is the measurement of double polarization spin observables in photoreactions on the proton, neutron, and deuteron. For instance, the beam-target double polarization E asymmetry of the $\vec{\gamma}\vec{d} \to \pi^0 np$ reaction at photon lab energy $E_\gamma = 349 \pm 5$ MeV has been recently measured [8]—see Eq. (7) for the definition of E asymmetry. This asymmetry will certainly provide an important test that, indirectly, allows us to check our knowledge on the process of pion production from the neutron. To the best of our

*darwish@sci.sohag.edu.eg; Corresponding author. Fax:+20 93 4601159.
†Present address: Grupo de Física Nuclear, Departamento de Física Atómica, Molecular y Nuclear, Facultad de Ciencias Físicas, Universidad Complutense de Madrid, Avda. Complutense s/n, E-28040 Madrid, Spain.

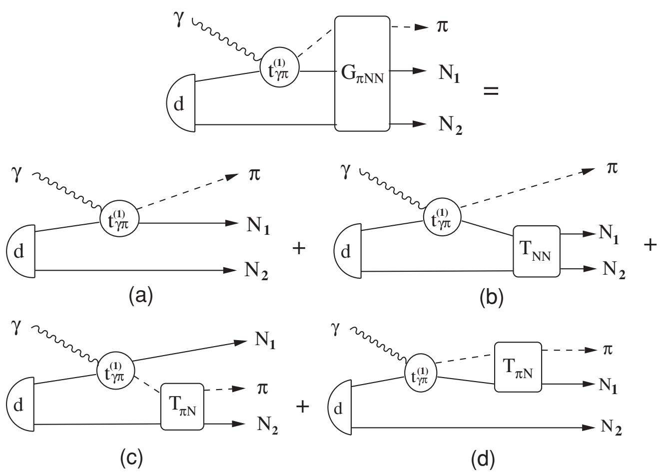

FIG. 1. Diagrammatic representation of the $\gamma d \to \pi NN$ amplitude including rescattering contributions in the two-body subsystems and neglecting all contributions of two-body meson-exchange currents. (a) Impulse approximation (IA); (b, c, and d) "driving terms" from NN and πN rescattering, respectively. Diagrams when the elementary pion photoproduction operator acts on nucleon 2 are not shown in the figure but are included in the calculations. In the calculations, each diagram shown in the figure goes accompanied by the diagram obtained by the exchange $N_1 \leftrightarrow N_2$.

knowledge, there is no calculation in the literature for the double polarization E asymmetry of the $\vec{\gamma}\vec{d} \to \pi NN$ reaction channels.

The helicity structure of quasifree pion photoproduction from the deuteron was studied in Refs. [10–12]. In Ref. [10], special emphasis was given to the beam-target spin asymmetry and the corresponding GDH sum rule for the deuteron, including complete hadronic rescattering in the NN and πN subsystems. The helicity dependence of the $\vec{d}(\vec{\gamma}, \pi^-)pp$ reaction channel was investigated in Ref. [11] with just the inclusion of NN rescattering in the final state. In that work, the differential polarized cross-section difference for parallel and antiparallel helicity states was predicted and the contribution of the $\vec{d}(\vec{\gamma}, \pi^-)pp$ channel to the deuteron spin asymmetry was evaluated. It was found that the effects of final state interactions (FSI) are larger in the asymmetry than in the unpolarized cross sections, which leads to a sizeable reduction of the deuteron spin asymmetry in the position of the peak. Both approaches [10,11] were restricted to the $\Delta(1232)$-resonance region in view of a relatively simple elementary pion photoproduction operator based on an effective Lagrangian approach from Ref. [13] that included only Born terms and the $\Delta(1232)$ resonance.

Later on, the work in Ref. [10] was improved by Arenhövel, Fix, and Schwamb in Ref. [12], where a better elementary production operator provided by MAID model [14] was employed and FSI effects were considered. Explicit evaluation of the deuteron spin asymmetry and the associated GDH sum rule were presented in said work.

In this article we present the first calculation for the $d(\gamma, \pi)NN$ reaction channels with polarized photon beam and polarized deuteron target in the near-threshold region.

The ultimate goal of the present article is to extend our approach, recently presented in Ref. [1], to make theoretical predictions for the helicity dependence in total and differential photoabsorption cross sections of the processes $\vec{\gamma}\vec{d} \to \pi^- pp$, $\vec{\gamma}\vec{d} \to \pi^+ nn$, and $\vec{\gamma}\vec{d} \to \pi^0 np$, in the energy range from threshold up to the $\Delta(1232)$ resonance, using as elementary $\gamma N \to \pi N$ reaction a realistic effective Lagrangian approach (ELA) from Refs. [15,16]. This elementary reaction model displays chiral symmetry, gauge invariance, and crossing symmetry, as well as a consistent treatment of the interaction with spin-3/2 particles. It also provides a reliable description of the threshold region. In this article we provide a theoretical overview of the double polarization E asymmetry for different pion photoproduction channels and we explicitly evaluate the contribution from separate channels to the GDH sum rule for the deuteron. It was found in Ref. [1] that the results for single-spin asymmetries are strongly dependent on the elementary pion photoproduction operator. Hence, we also investigate the sensitivity of the double-spin polarization observables to the elementary $\gamma N \to \pi N$ operator.

The calculations presented in this article are of high interest in view of the extensive recent polarization measurements from the A2 and GDH@MAMI [6] and LEGS@BNL [8] Collaborations. A theoretical understanding of these data on the deuteron target will provide information about the pion photoproduction from the neutron reaction, which is not well known yet, but is required for a complete understanding of Δ excitations in the pion photoproduction process.

In Sec. II we briefly review the general formalism for the $d(\gamma, \pi)NN$ reaction [1,4]. Results for the $\vec{\gamma}\vec{d} \to \pi^- pp$, $\vec{\gamma}\vec{d} \to \pi^+ nn$, and $\vec{\gamma}\vec{d} \to \pi^0 np$ reactions are presented and discussed in Sec. III. Finally, we provide conclusions in Sec. IV.

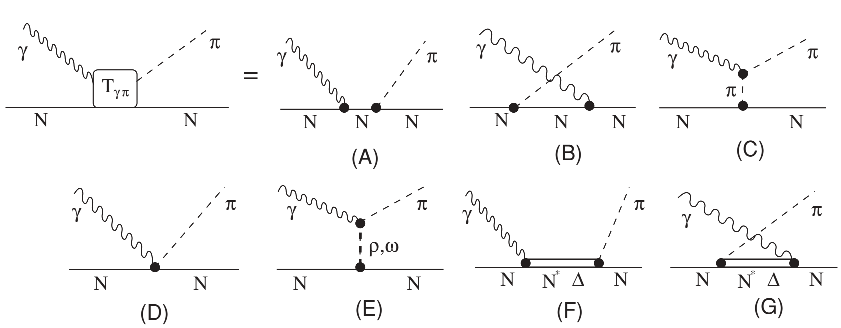

FIG. 2. Feynman diagrams for pion photoproduction from free nucleons. Born terms: (A) direct nucleon pole or s channel, (B) crossed nucleon pole or u channel, (C) pion in flight or t channel, and (D) Kroll-Rudermann contact term; (E) vector-meson exchange (ρ and ω); resonance excitations contribution: (F) direct or s channel and (G) crossed or u channel.

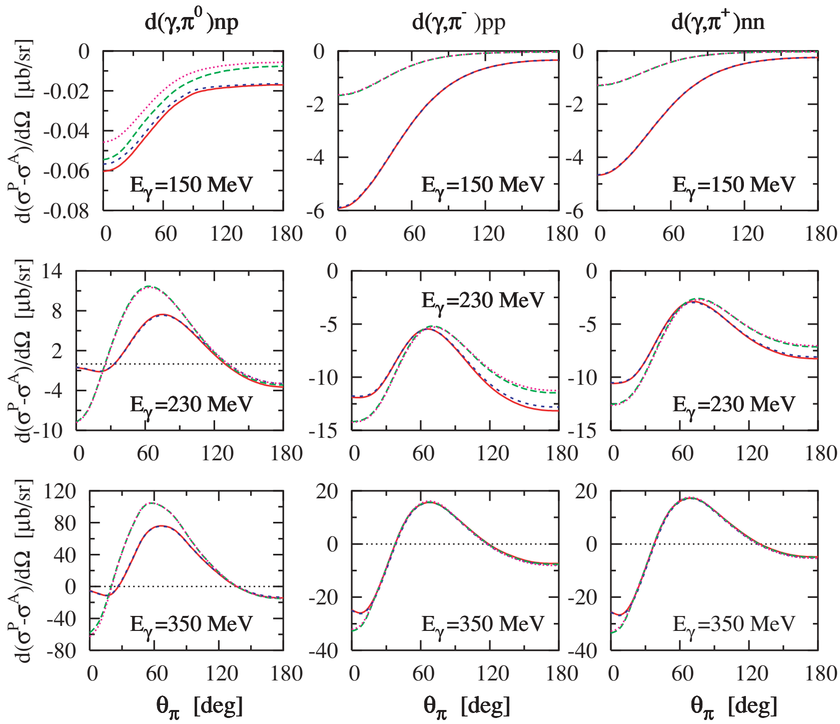

FIG. 3. (Color online) Circular photon polarization asymmetry for the separate channels of semiexclusive pion photoproduction on the deuteron as a function of the pion angle in the laboratory frame at various photon lab energies using the electromagnetic multipoles of set no. 2 from the effective Lagrangian approach in Refs. [15,16]. Curve conventions: (dotted) IA; (long-dashed) IA+πN; (short-dashed) IA+NN; (solid) IA+NN+πN.

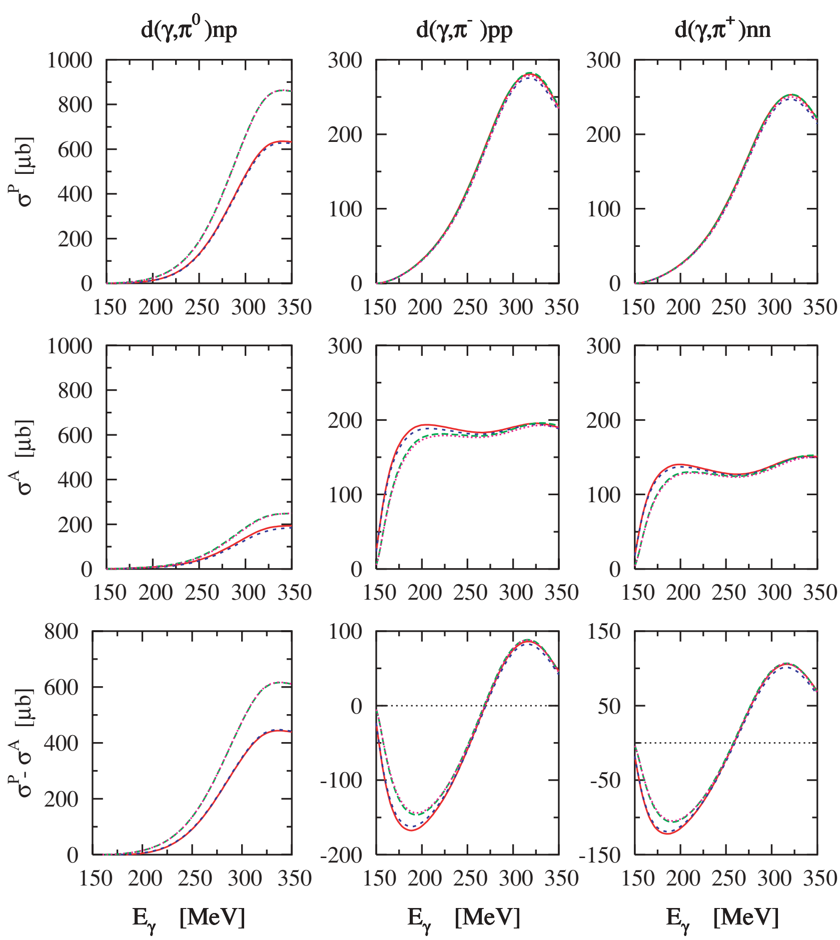

FIG. 4. (Color online) The helicity-dependent total photoabsorption cross sections for the separate channels of $\vec{d}(\vec{\gamma},\pi)NN$ for circularly polarized photons on a longitudinally polarized deuteron with spin parallel σ^P (upper panel) and antiparallel σ^A (middle panel) to the photon spin in the energy region from threshold up to the $\Delta(1232)$ resonance. The lower panel shows the difference $\sigma^P - \sigma^A$, i.e., the deuteron spin asymmetry of total photoabsorption cross section. Curve conventions as described in the caption to Fig. 3.

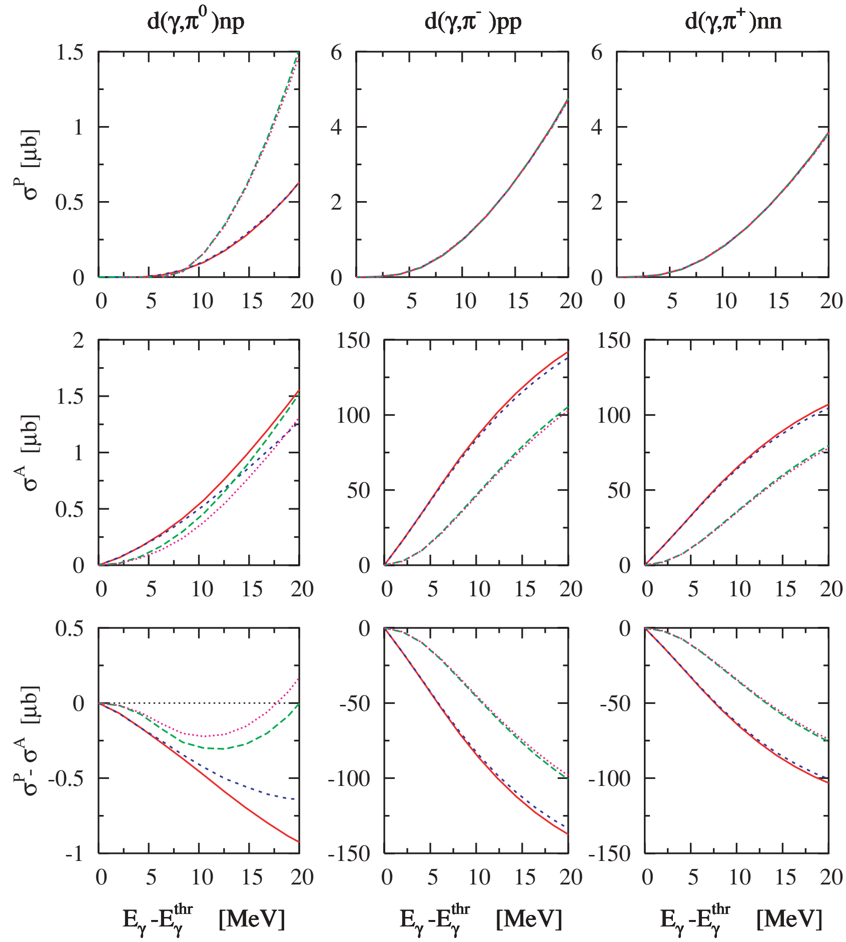

FIG. 5. (Color online) Same as in Fig. 4 but in the energy region near threshold. $E_\gamma - E_\gamma^{\mathrm{thr}}$ denotes the excess energy above threshold in the laboratory system.

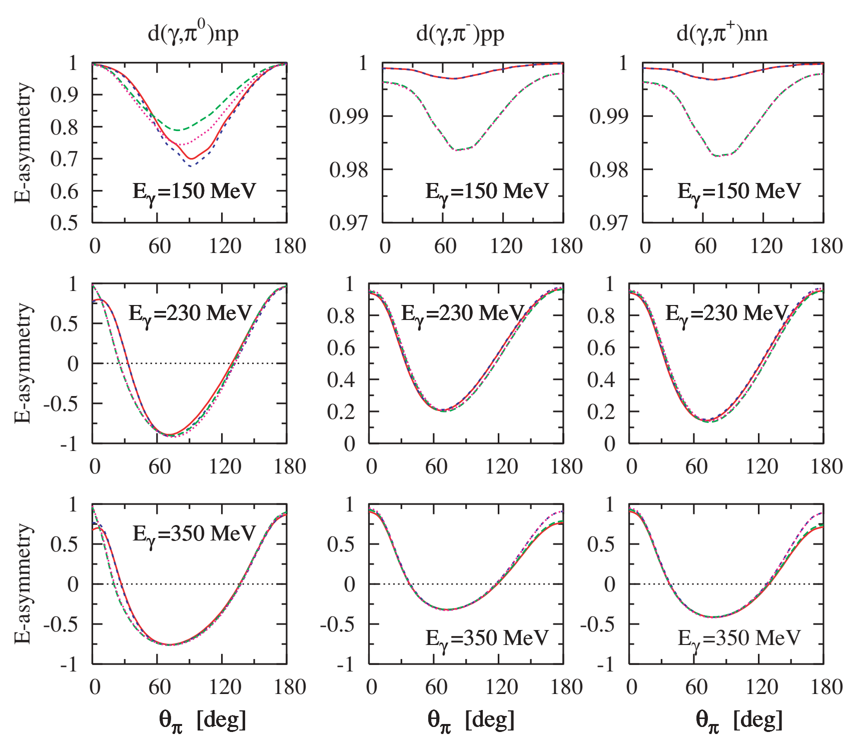

FIG. 6. (Color online) The double polarization E asymmetry [see Eq. (7) for its definition] as a function of the pion angle in the laboratory frame at various photon lab energies for the separate channels of the reaction $\vec{d}(\vec{\gamma},\pi)NN$ for circularly polarized photons on a longitudinally polarized deuteron. Curve conventions as in Fig. 3.

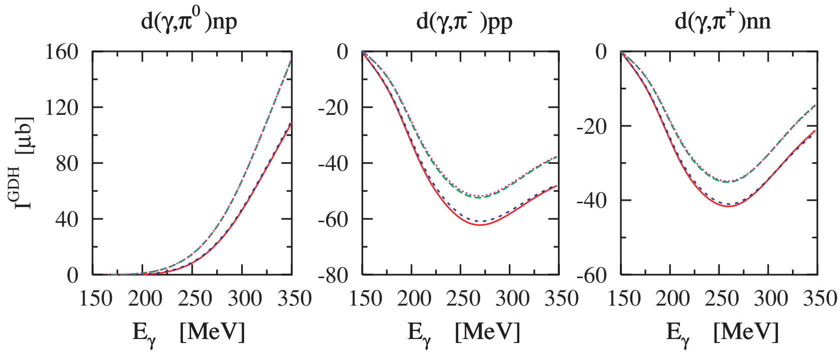

FIG. 7. (Color online) The Gerasimov-Drell-Hearn integral [see Eq. (9) for its definition] as a function of the upper integration limit for separate channels of the $\vec{d}(\vec{\gamma},\pi)NN$ reaction. Curve conventions as in Fig. 3.

II. FORMALISM

We start with a brief description of the basic formal ingredients of quasifree pion photoproduction reaction from the deuteron

$$\gamma(k,\vec{\varepsilon}_\mu)+d(d)\to\pi(q)+N_1(p_1)+N_2(p_2), \tag{1}$$

where the four-momenta of the involved particles are indicated within parentheses. In Fig. 1 we present the Feynman diagrams of the scattering matrix for reaction (1). Full treatment of all interaction effects requires, in principle, a full unitary πNN three-body calculation. In the present work, however, we restrict ourselves to the inclusion of complete rescattering in the various two-body subsystems of the final state [Figs. 1(b), 1(c), and 1(d)]. The treatment follows previous works [1,4], to which the reader is referred for formal details.

The three contributions in Figs. 1(a)–1(d) present three different contributions to the reaction amplitude. We refer to them as (a) impulse approximation (IA); (b) the NN-rescattering contribution; and (c) πN_c-rescattering and (d) the πN_d-rescattering contributions. The total transition matrix element reads

$$T_{sm\,\mu m_d}=T^{IA}_{sm\,\mu m_d}+T^{NN}_{sm\,\mu m_d}+T^{\pi N_{(c)+(d)}}_{sm\,\mu m_d}. \tag{2}$$

The starting point of our formalism is the IA [Fig. 1(a)], which is completely determined by the elementary amplitude $\gamma N\to\pi N$ and the deuteron wave function as follows

$$T^{IA}_{sm\,\mu m_d}=\sum_{m'}[\langle sm\,|\langle\vec{p}_1|t_{\gamma\pi}(W_{\gamma N_1})|-\vec{p}_2\rangle \times\phi_{m'm_d}(\vec{p}_2)|\,1\,m'\rangle-(1\leftrightarrow 2)], \tag{3}$$

where $t_{\gamma\pi}$ denotes the elementary pion photoproduction operator on the free nucleon; $W_{\gamma N_1}$ the invariant energy of the γN_1 system; $\vec{p}_1=(\vec{k}-\vec{q})/2+\vec{p}$, and $\vec{p}_2=(\vec{k}-\vec{q})/2-\vec{p}$. $\phi_{mm_d}(\vec{p}\,)$ is given by

$$\phi_{mm_d}(\vec{p}\,)=\sum_{L=0,2}\sum_{m_L} i^L C^{L\,1\,1}_{m_L\,m\,m_d}u_L(p)\,Y_{Lm_L}(\hat{p}) \tag{4}$$

and we compute the radial deuteron wave function $u_L(p)$ using the realistic Paris potential [17].

The contribution from NN rescattering [Fig. 1(b)] to the transition matrix is

$$T^{NN}_{sm\mu m_d}=\langle\vec{q},\vec{p},sm\,|\,\mathcal{T}_{NN}G_{NN}\big[t^{(1)}_{\gamma\pi}(W_{\gamma N_1})+t^{(2)}_{\gamma\pi}(W_{\gamma N_2})\big]|\,1\,m_d\rangle, \tag{5}$$

where $\mathcal{T}_{NN}$ stands for the half-off-shell NN-scattering matrix and G_{NN} for the corresponding free NN propagator. The former is obtained from separable representation of a realistic NN interaction [18], including all S, P, and D partial waves.

Similarly to the NN matrix element, we obtain the πN-rescattering contribution [Figs. 1(c) and 1(d)]

$$T^{\pi N_{(c)+(d)}}_{sm\mu m_d}=\sum_{j=c,d}\langle\vec{q},\vec{p},sm|\,\mathcal{T}_{\pi N_j}G_{\pi N_j}\big[t^{(1)}_{\gamma\pi}(W_{\gamma N_1})+t^{(2)}_{\gamma\pi}(W_{\gamma N_2})\big]|\,1\,m_d\rangle, \tag{6}$$

where we calculate the half-off-shell πN-scattering matrix $\mathcal{T}_{\pi N}$ from a separable energy-dependent πN potential [19], including all S to D waves. The explicit formal expressions for the three contributions in Eqs. (3), (5), and (6) can be found in Refs. [1,4] and we refer to these article for details.

For the evaluation of Eqs. (3), (5), and (6) one has also to specify the elementary pion photoproduction operator for

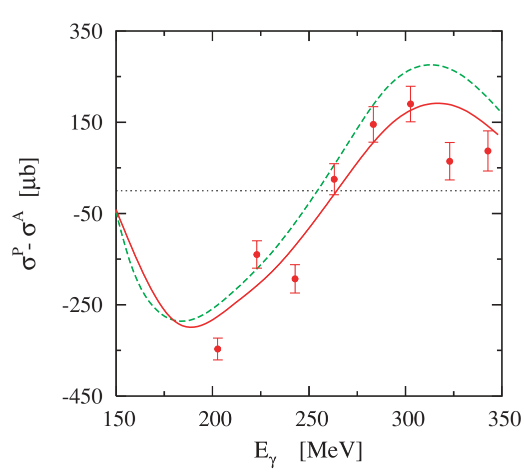

FIG. 8. (Color online) The helicity-dependent total photoabsorption cross section difference $(\sigma^P-\sigma^A)$ for the semiexclusive channels $\vec{\gamma}\vec{d}\to\pi^\pm NN$. Curve conventions: (dashed) IA*+NN+πN_c using MAID [14]; (solid) IA+NN+πN using the bare electromagnetic multipoles of ELA [15,16,20]. Experimental data are taken from Ref. [7].

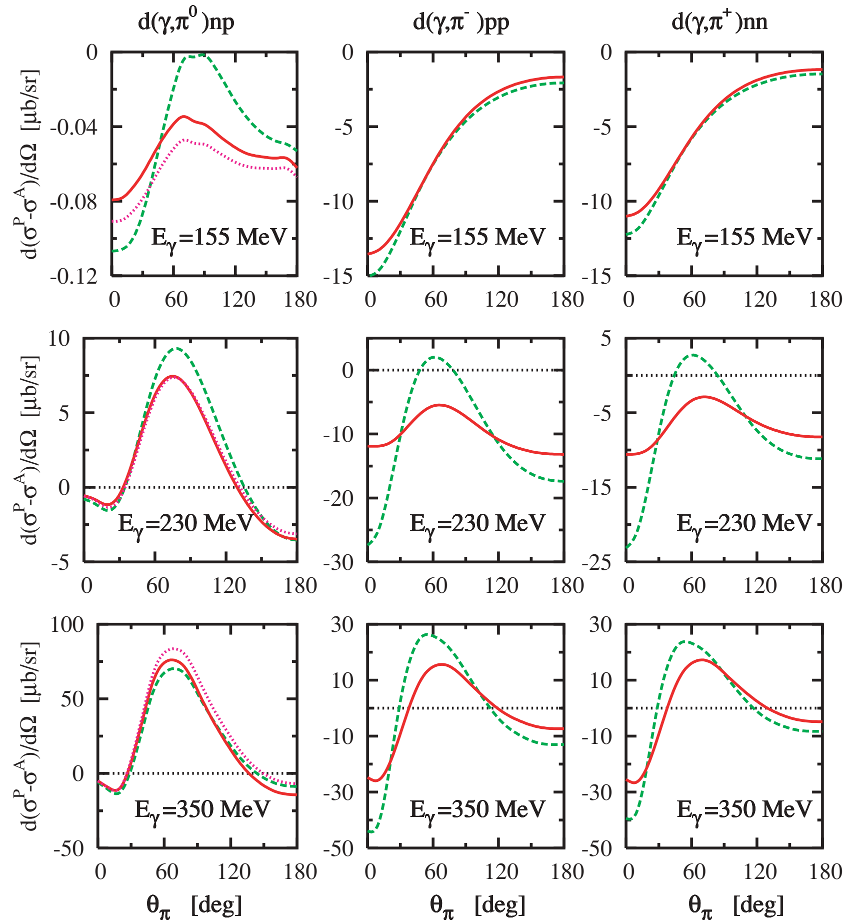

FIG. 9. (Color online) Circular photon polarization asymmetry for the separate channels of semiexclusive pion photoproduction on the deuteron as a function of the pion angle in the laboratory frame at various photon lab energies using different elementary pion photoproduction operators and including FSI effects. Curve conventions: (dashed) $IA^*+NN+\pi N_c$ using MAID [14]; (dotted) $IA^*+NN+\pi N_c$ using the dressed multipoles of ELA [15,16,20]; (solid) $IA+NN+\pi N$ using the bare electromagnetic multipoles of ELA.

the $N(\gamma,\pi)N$ reaction. As stated in the Introduction, we use a realistic elementary operator from Refs. [15,16,20]. This model has been successfully applied to the $N(\gamma,\pi)N$ process from threshold to 1 GeV of photon energy in the laboratory reference system. The model is based on an effective Lagrangian approach that, from a theoretical point of view, is an appealing, reliable, and formally well-established approach in the energy region of the mass of the nucleon. The model includes Born terms [Figs. 2(A)–2(D)], vector-meson exchanges [ρ and ω, in Fig. 2(E)], and all the four star resonances in the Particle Data Group (PDG) [21] up to 1.7 GeV and up to spin-3/2: $\Delta(1232)$, $N(1440)$, $N(1520)$, $N(1535)$, $\Delta(1620)$, $N(1650)$, and $\Delta(1700)$ [Fig. 2(F) and 2(G)]. In Ref. [15] the single and double polarization asymmetries for pion photoproduction from free nucleons were computed and compared to the available experimental database. The agreement with data was found to be fairly good. Recently, the model has also been applied successfully to η photoproduction from the proton [22].

The model displays chiral symmetry, gauge invariance, and crossing symmetry as well as a consistent treatment of the spin-3/2 interaction that overcomes pathologies present in former analyses [23]. The dressing of the resonances is considered by means of a phenomenological width that contributes to both s and u channels and takes into account decays into one π, one η, and two π. In the pion photoproduction model from free nucleons [15,16] it was assumed that FSI factorize and can be included through the distortion of the πN final state wave function (pion-nucleon rescattering). πN-FSI was included [15,16] by adding a phase $\delta_{\rm FSI}$ to the electromagnetic multipoles. This phase is set so that the total phase of the multipole matches the total phase of the energy dependent solution of SAID [24]. In this way it was possible to isolate the contribution to the physical observables from the bare diagrams. The parameters of the resonances were extracted from data fitting the electromagnetic multipoles of the energy-independent solution of SAID [24], applying a modern optimization technique based on genetic algorithms combined with gradient-based routines [16,22,25] that provide reliable values for the parameters of the nucleon resonances. Once the bare properties of the nucleon resonances have been extracted from data, their contribution to other processes can be calculated. For further details on the model we refer the reader to Refs. [1,15,16,20].

III. RESULTS AND DISCUSSION

We divide into four parts the discussion of the results obtained. First, we report results on the doubly polarized differential and total cross sections for the parallel and antiparallel helicity states of the $\vec{\gamma}\vec{d} \to \pi^0 np$, $\vec{\gamma}\vec{d} \to \pi^- pp$, and $\vec{\gamma}\vec{d} \to \pi^+ nn$ processes in the energy region from threshold up to the $\Delta(1232)$ resonance. The contribution of these processes to the spin response of the deuteron, i.e., the asymmetry

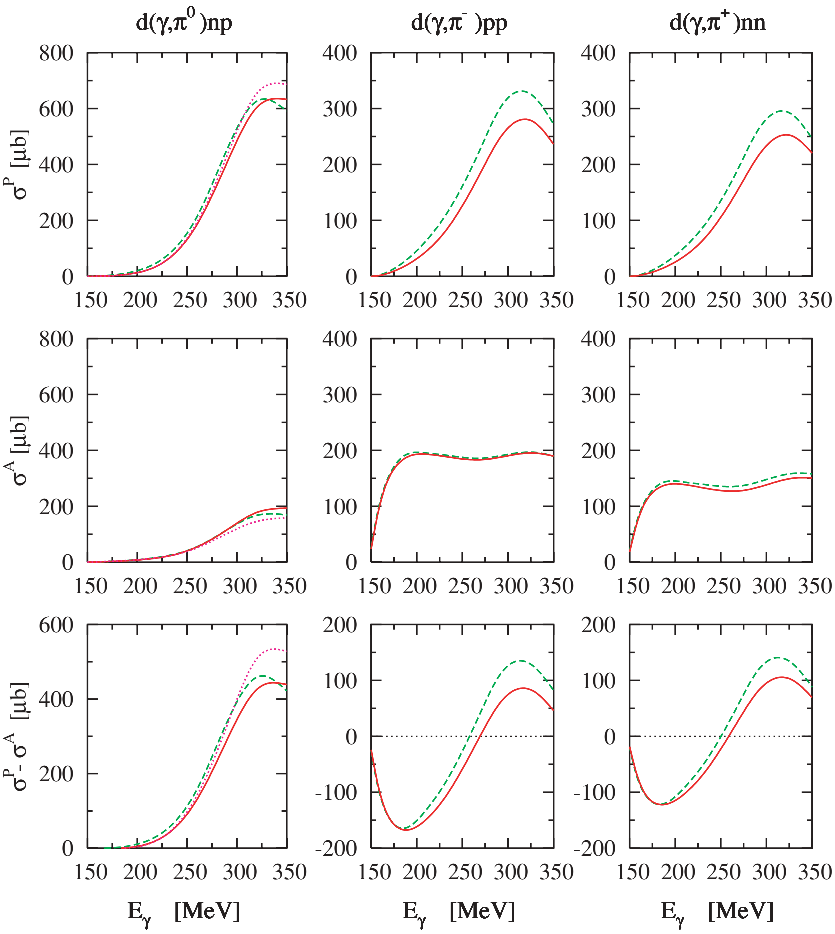

FIG. 10. (Color online) Total photoabsorption cross sections for the separate channels of $\vec{d}(\vec{\gamma},\pi)NN$ for circularly polarized photons on a longitudinally polarized deuteron with spin parallel σ^P (upper part) and antiparallel σ^A (middle part) to the photon spin using different elementary operators and including FSI effects. The lower part shows the difference $\sigma^P - \sigma^A$. Curve conventions as described in the caption to Fig. 9.

of the total photoabsorption cross section with respect to parallel and antiparallel spins of photon and deuteron, is explicitly evaluated in this part. The second part is devoted to the results for the beam-target double polarization E asymmetry, whereas in the third part, the contribution of the separate pion photoproduction channels to the deuteron GDH integral is evaluated by explicit integration up to a photon lab-energy of $E_\gamma = 350$ MeV. In the last one,we discuss the sensitivity of our results to the elementary $\gamma N \to \pi N$ amplitude.

In the figures we compare calculations with different ingredients. We display separately the contributions from the bare and the final-state interactions. We call impulse approximation (IA) to the contribution to the observables shown in Fig. 1(a) using the bare electromagnetic multipoles together with the same diagram exchanging $N_1 \leftrightarrow N_2$. In what follows, when we cite Figs. 1(a)–1(d) we implicitly mean the contributions of both the depicted diagram and the corresponding one obtained under $N_1 \leftrightarrow N_2$ exchange.

As we stated in our preceding article [1], one has to be careful with what one calls IA. We would like to explain carefully what we call IA and how we compute it. A truly IA calculation [a calculation that includes only Fig. 1(a)] cannot employ directly the elementary amplitudes that fit the data on electromagnetic multipoles for the $\gamma N \to \pi N$ process. This is due to the fact that πN rescattering is unavoidably included in the "elementary" amplitude in these fits to data. For example, if we use the multipoles provided by the ELA model that fits the experimental data, and afterwards we include πN rescattering between the pion and the spectator nucleon, we are not really including just Figs. 1(a)+1(c) but rather Figs. 1(a)+1(c)+1(d), with a contribution of πN rescattering of the pion with the knocked-out nucleon that comes from the photoproduction operator. For the same reason computations in Refs. [3,4,10,12] implicitly include to some extent Fig. 1(d), although it is not explicitly considered, and a certain content of such diagram is also present in the rest of the calculated rescattering terms.

Therefore, if we wish to calculate the contribution coming just from Fig. 1(a), the bare IA contribution to the amplitude has to be extracted from the analysis of the $\gamma N \to \pi N$, where the final-state interaction has to be removed. This was done in Refs. [15,16]. We name the calculations where the πN rescattering is included in the elementary reaction IA*. IA* is, therefore, somehow equivalent to a Fig. 1(a)+1(d) calculation. In Sec. III D we compare results for IA*+rescattering and IA+rescattering results using MAID and ELA models and, thus, we survey the effects of πN rescattering and the influence of the basic pion production operator. We refer to the inclusion of Fig. 1(a) in a calculation as IA, to the inclusion of diagram (b) as NN, and to the inclusion of Figs. 1(c)+1(d), using the πN rescattering explained in this article, as πN. When only Fig. 1(c) is accounted for in the πN rescattering it is labeled πN_c.

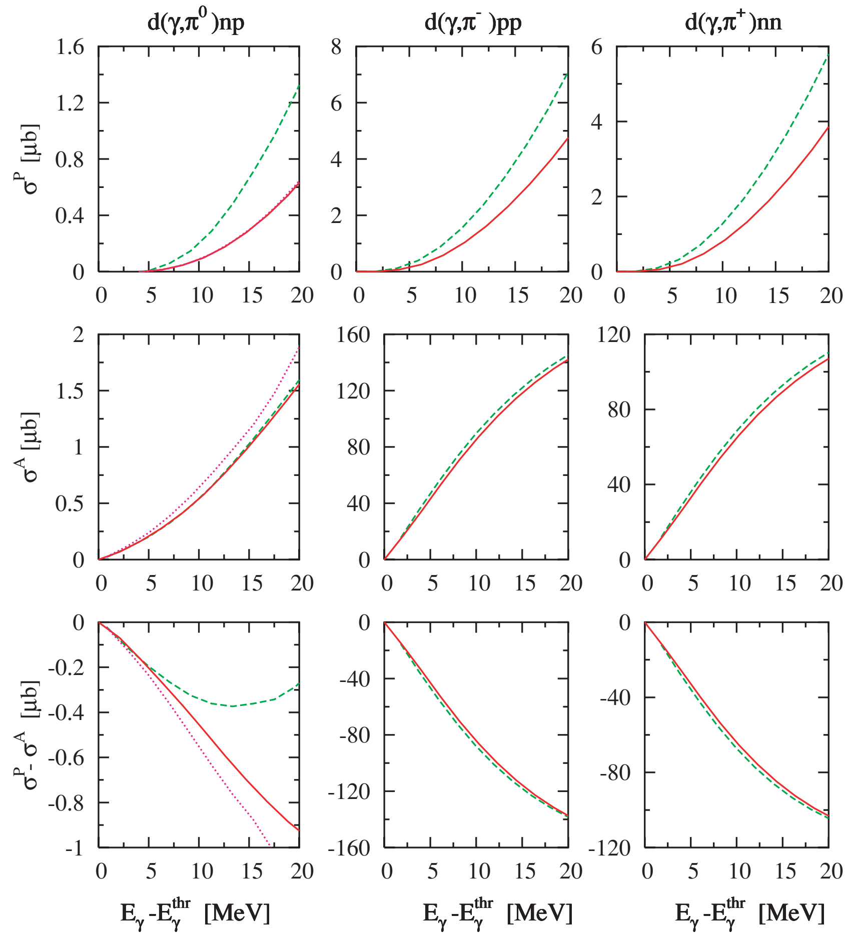

FIG. 11. (Color online) Same as in Fig. 10 but in the near-threshold region.

The full consistent calculation with all the effects considered in this work is what we refer to as IA+πN+NN.

A. Helicity dependent cross sections

First, we present results for the semiexclusive differential spin asymmetry $d(\sigma^P - \sigma^A)/d\Omega$ with respect to circularly polarized photons, where $P(A)$ stands for the deuteron spin oriented parallel (antiparallel) to the photon spin. In Fig. 3 we depict results for the pure IA calculation as well as with the inclusion of rescattering effects, for the individual pion photoproduction channels. We have chosen three laboratory photon energies covering the region from near threshold to the $\Delta(1232)$ resonance. This spin asymmetry has been measured by the A2 and GDH Collaborations at MAMI [6].

The importance of rescattering in the neutral channel is clearly addressed when the full (IA $+ NN + \pi N$) and the IA calculations are compared (respectively, solid and dotted curves in Fig. 3). We observe that the πN rescattering is not very important in both neutral and charged channels and that the NN rescattering plays a central role. Only at energies close to threshold, a small influence of πN-FSI is observed. This means, in particular, that the helicity asymmetry $d(\sigma^P - \sigma^A)/d\Omega$ at photon energies near threshold is sensitive to the choice of the elementary reaction amplitude and the πN-rescattering. In charged channels, we find that FSI rescattering is quite small, and indeed almost negligible at pion backward angles and energies near the $\Delta(1232)$ region. It is due to the fact that in charged-pion production the $^3S_1$ contribution to the NN final state is forbidden.

The results for the doubly polarized total cross sections in the case of the IA alone and with FSI effects are shown in Fig. 4 (from threshold up to the $\Delta(1232)$-resonance region) and Fig. 5 (near threshold region). Results are displayed in Figs. 4 and 5 as follows: (upper panel) total photoabsorption cross sections σ^P for circularly polarized photons on a target with spin parallel to the photon spin; (middle panel) σ^A, the same for antiparallel spins of photon and deuteron target; (lower panel) spin asymmetry $\sigma^P - \sigma^A$ for the individual contributions of the different pion charge states to the $\vec{\gamma}\vec{d} \rightarrow \pi NN$ reaction. Several experiments to measure the deuteron spin asymmetry are presently underway [6]. In these experiments, deuterium serves as a neutron target and quasifree kinematics are preferred to minimize possible interaction effects.

The left panels in Figs. 4 and 5 show the importance of rescattering effects in the neutral channel when the full calculation (solid curve) is compared to the IA one (dotted curve). The most important contribution to FSI comes from NN rescattering, whereas πN rescattering is much smaller and is significative only in σ^A at photon energies close to threshold in the neutral channel (see the left panel in Fig. 5). This is due to the nonorthogonality of the final-state plane wave in IA to the deuteron bound-state wave function. We

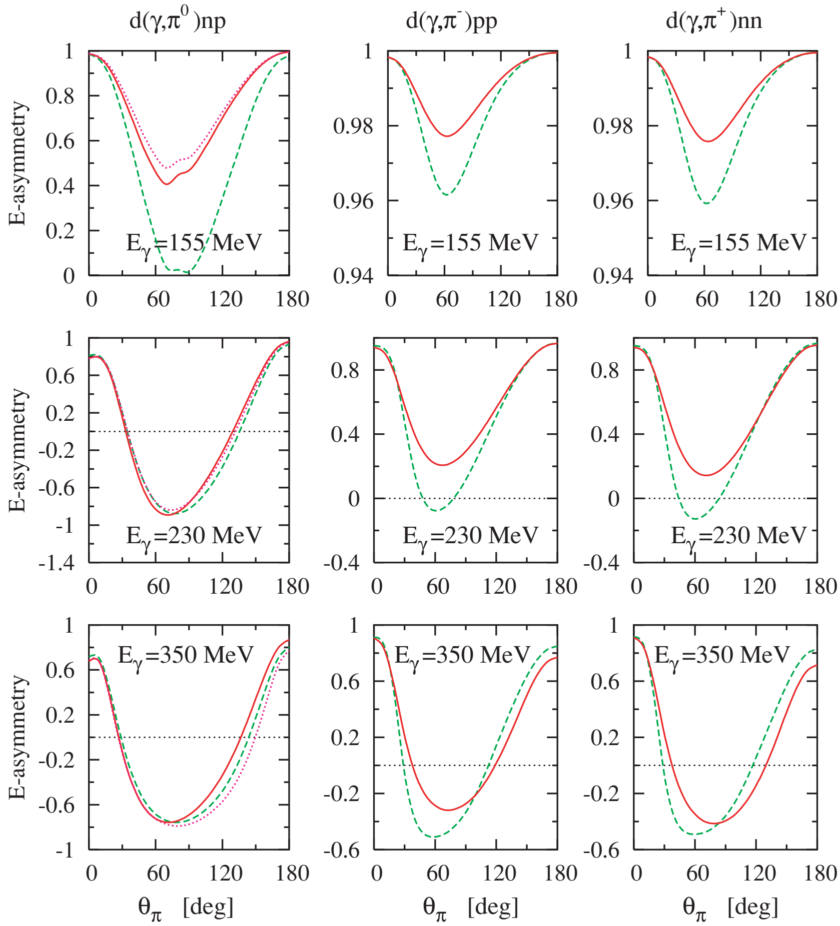

FIG. 12. (Color online) The double polarization E asymmetry as a function of the pion angle in the laboratory frame at various photon lab energies for the separate channels of $\vec{d}(\vec{\gamma},\pi)NN$ using different elementary pion photoproduction operators and including FSI effects. Curve conventions as in Fig. 9.

also find that FSI effects are equally important for both σ^P and σ^A. FSI effects lead to an overall strong reduction of the spin asymmetry in the energy region of the $\Delta(1232)$ resonance. σ^P is larger than σ^A because of the $\Delta(1232)$ excitation.

The cross sections σ^P and σ^A as well as the spin asymmetry $\sigma^P - \sigma^A$ present qualitative and quantitatively similar behaviors for both charged pion production channels. The FSI effects appear mainly in σ^A at photon lab energies close to threshold (Fig. 5). We find that the spin asymmetry $\sigma^P - \sigma^A$ starts out negative due to the E_{0+} multipole, which is dominant in the threshold region and has a strong positive contribution at higher energies due to the M_{1+} multipole, which is dominant in the $\Delta(1232)$-resonance region. The effect of FSI is important for both the neutral and charged pion production channels in the threshold region.

B. The double polarization E asymmetry

As already mentioned in the Introduction, there is a great deal of interest in experiments [8] to determine the beam-target double polarization E asymmetry for the $\vec{\gamma}\vec{d} \to \pi NN$ reaction channels. In connection with this study, we provide in Fig. 6 a sample of E asymmetry as a function of the emission pion angle θ_π in the laboratory frame for the individual pion photoproduction channels. This asymmetry is given by

$$E(\theta_\pi) = \frac{d(\sigma^A - \sigma^P)/d\Omega}{d(\sigma^A + \sigma^P)/d\Omega} = \frac{d(\sigma^A - \sigma^P)/d\Omega}{2(d\sigma_0/d\Omega)}, \qquad (7)$$

where $d\sigma^P/d\Omega$ and $d\sigma^A/d\Omega$ represent the spin parallel and antiparallel differential cross sections, respectively, and $d\sigma_0/d\Omega$ denotes the unpolarized differential cross section. The helicity dependent cross sections are well suited to verify the GDH sum rule, to do partial channel analysis, and to give contributions to the double polarization E asymmetry. This asymmetry appears as an interference between the amplitudes with different parity-exchange properties.

The helicity E asymmetry (Fig. 6) has qualitatively a similar behavior for all pion photoproduction channels. The maximum value of E equals unity at $\theta_\pi = 0^\circ$ and 180°. The curves begin with unity and decrease as the pion angle increases until the minimum value is reached at $\theta_\pi \simeq 90^\circ$. Then, it increases again to unity. The negative values in the E asymmetry come from higher positive contribution in $d\sigma^P/d\Omega$.

Figure 6 shows also that the helicity E asymmetry does not exhibit a strong effect of the rescattering contribution and, therefore, it is an excellent observable to test any weakness in the underlying elementary reaction model. We find that FSI are sizable in the neutral channel, whereas in charged channels they are noticeable only at the lowest energy. The E asymmetry proves to be sensitive to the choice of the input

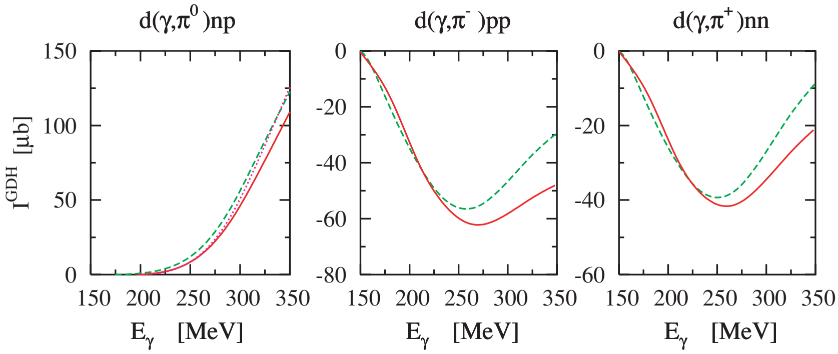

FIG. 13. (Color online) The Gerasimov-Drell-Hearn integral as a function of the upper integration limit for separate channels of the $\vec{d}(\vec{\gamma},\pi)NN$ reaction using different elementary pion photoproduction operators and including FSI effects. Curve conventions as in Fig. 9.

elementary $\gamma N \to \pi N$ amplitude and the πN rescattering (see Sec. III D). We would like to point out that very preliminary data for the helicity E asymmetry of the $\vec{\gamma}\vec{d} \to \pi^0 np$ reaction at photon lab energy $E_\gamma = 349 \pm 5$ MeV were measured by the LEGS@BNL Collaboration [8]. However, the data analysis has not yet been completed.

C. The Gerasimov-Drell-Hearn integral

Next, we discuss the GDH sum rule [9] which links the anomalous magnetic moment of a particle to the energy weighted integral of the spin asymmetry of the photoabsorption cross section. For a particle of mass M, charge eQ, anomalous magnetic moment κ, and spin S it reads

$$I^{\text{GDH}} = \int_0^\infty \frac{dE'_\gamma}{E'_\gamma}\left[\sigma^P(E'_\gamma) - \sigma^A(E'_\gamma)\right] = 4\pi^2\kappa^2\frac{e^2}{M^2}S, \quad (8)$$

where $\sigma^{P(A)}$ denote the total absorption cross sections for circularly polarized photons on a target with spin parallel (P) and antiparallel (A) to the photon spin. This sum rule provides a very interesting relation between a ground-state property (κ) of a particle and its whole excitation spectrum. Apart from the general assumption that the integral in Eq. (8) converges, its derivation is based solely on first principles like Lorentz and gauge invariances, unitarity, crossing symmetry, and causality of the Compton scattering amplitude of a particle. Consequently, from the experimental and theoretical points of view, a test for various targets becomes of great interest.

To present the results in a direct way, we introduce the finite GDH integral as defined by

$$I^{\text{GDH}}(E_\gamma) = \int_0^{E_\gamma} \frac{dE'_\gamma}{E'_\gamma}[\sigma^P(E'_\gamma) - \sigma^A(E'_\gamma)]. \quad (9)$$

In Fig. 7 we depict our results for the evaluation of the GDH integral for the individual contributions from the different charge states of the pion for the $\gamma d \to \pi NN$ reaction as a function of the upper integration limit. The contributions of various pion photoproduction channels to the finite GDH integral [Eq. (9)] up to 350 MeV and their sum are summarized in Table I.

We find that a large positive contribution to the value of the deuteron GDH integral (integrated up to 350 MeV) comes from the π^0-photoproduction channel, whereas the charged pion channels give a negative but—in absolute value—smaller contribution to the value of the deuteron GDH integral. The inclusion of NN rescattering reduces significantly (more than a half, see Table I) the total value of the deuteron GDH integral up to 350 MeV from its IA value. This sizable reduction is due to the nonorthogonality of the final-state plane wave in impulse approximation to the deuteron bound-state wave function. The integral is then further slightly reduced by the πN-rescattering. Contrary with what we have found in other observables presented in this article, we find that FSI effects are sizable in the GDH integral for both neutral and charged pion production channels. The measurement of spin asymmetry for the various pion photoproduction channels on the deuteron represents a stringent test of our present theoretical understanding of the $\gamma d \to \pi NN$ reaction. Hence, the experimental programs at facilities like MAMI at Mainz and ELSA at Bonn, concerning the GDH sum rule on the deuteron are of great importance for further progress in the field.

D. Sensitivity to the $\gamma N \to \pi N$ amplitude

In what follows, we discuss the influence of different choices for the input elementary pion photoproduction operator on the results presented above for the $\vec{\gamma}\vec{d} \to \pi NN$ reaction channels. In a recent exploratory study, we have investigated the role of these choices on the unpolarized cross sections and single-spin asymmetries [1]. During the present study we restrict ourselves to compare results for double-polarization asymmetries and the GDH sum rule for the deuteron in the energy region from near threshold to the $\Delta(1232)$ resonance, using as elementary reaction amplitudes the ones provided by the ELA model from [15,16] and those obtained using MAID model [14]. The results of this comparison are collected in Figs. 8–13.

First, in Fig. 8 we show the helicity-dependent total photoabsorption cross-section difference $(\sigma^P - \sigma^A)$ for the

TABLE I. Contributions of various channels for quasifree pion photoproduction from the deuteron to the finite GDH integral using the elementary reaction from Refs. [15,16] and explicitly integrated up to a photon lab energy of $E_\gamma = 350$ MeV in μb.

Contribution	$\pi^- pp$	$\pi^+ nn$	$\pi^0 np$	πNN
IA	−36.08	−13.07	155.93	106.78
IA+NN	−46.28	−20.37	111.04	44.39
IA+NN+πN	−47.76	−20.11	109.16	41.29

TABLE II. Same as Table I but using the MAID model [14] as elementary reaction operator.

Contribution	$\pi^- pp$	$\pi^+ nn$	$\pi^0 np$	πNN
IA*	−23.02	−3.87	174.36	147.47
IA*+NN	−28.79	−8.65	123.13	85.69
IA* + NN+πN_c	−29.38	−8.68	122.67	84.61

semiexclusive channels $\vec{\gamma}\vec{d} \to \pi^\pm NN$ using the elementary operators from MAID (dashed curve) and our ELA model (solid curve), including FSI effects. We compare to the latest experimental data from the A2 and GDH@MAMI Collaborations [7] and we find an excellent agreement with data. Our ELA computation provides a slightly better agreement than the computation using MAID model.

In Fig. 9 we show the helicity differential cross-section difference $d(\sigma^P - \sigma^A)/d\Omega$ using the bare ELA model (solid), using MAID model (dashed) and the dressed ELA model (dotted) in the neutral channel. Both results are quite different, specially at low energies. At the peak position, we obtain larger values using MAID than using ELA. At extreme forward pion angles, large differencies between both results is obtained. This discrepancy is more noticeable for energies close to threshold and shows up the differences among elementary operators. The difference between the dotted (dressed ELA) and solid (bare ELA) curves shows the effect of πN rescattering, which is found to be important near threshold.

If we focus our attention on the helicity total cross sections as shown in Figs. 10 and 11, similar results are obtained. A sizable difference is obtained in the energy region near threshold. Considerable differences are seen also in the case of E asymmetry (Fig. 12) and GDH integral (Fig. 13). Table II displays the extracted values of the GDH integral up to 350 MeV for all three pion photoproduction channels and their sum for our results using MAID as elementary reaction operator. Compared the values in Table II using MAID to the values presented in Table I using ELA, we find that ELA: $I^{\rm GDH}_{IA}(350\,{\rm MeV}) = 106.78\ \mu$b, whereas MAID: $I^{\rm GDH}_{IA^*}(350\,{\rm MeV}) = 147.47\ \mu$b. After including FSI effects we obtained ELA: $I^{\rm GDH}_{IA+NN+\pi N}(350\ {\rm MeV}) = 41.29\ \mu$b, whereas MAID: $I^{\rm GDH}_{IA^*+NN+\pi N_c}(350\ {\rm MeV}) = 84.61\ \mu$b.

In the charged channels the results using MAID or ELA as elementary reaction operators are different in the near-threshold region, where the predicted E asymmetry within the ELA is—in negative sign—smaller than those within MAID but provides similar results in the $\Delta(1232)$ region. Although both computations provide results for the GDH integral that differ in, approximately, a factor 2, the curves computed using MAID and ELA models displayed in Fig. 8 are not much different, and one must look more in deep for the reasons in the different GDH values. This large difference in the GDH—in spite of the relatively small dissimilarity shown in Fig. 8—shows the large sensitivity of the GDH integral to the choice of the elementary operator employed. The GDH results from two large contributions of negative and positive signs, that cancel to a large extent in the final results. The curve computed with the MAID model seems more "symmetric" and hence the cancellation of the positive and the negative contributions to the integral is larger than for the ELA model computation, which presents a larger—in absolute value—negative part. This partial cancellation also means that the contribution of the processes considered in this work to the total GDH integral up to 350 MeV is relatively small compared to other contributions. For instance in Ref. [12] a value of about 240 μb for the total GDH integral up to 350 MeV is found. Our pionic contributions gives 42 μb. The rest should be either coherent pion production or two-nucleon breakup. Summarizing, we can say that the MAID model provides different predictions for polarization observables than the ELA model, particularly at low photon energies, and that the GDH integral provides an excellent observable to test different pion production operators.

From the preceding discussion it is apparent that πN rescattering and the choice of the elementary operator have a visible effect on spin observables. It is also so in certain single-spin asymmetries [1].

IV. SUMMARY AND CONCLUSIONS

The main topic of this article was the investigation of the helicity structure of the partial cross sections and their contributions to the spin asymmetries and the GDH sum rule for the deuteron. Contributions from various single-pion photoproduction channels have been explicitly evaluated in the energy region from near threshold up to photon lab energy of $E_\gamma = 350$ MeV, including all leading πNN effects. For the elementary operator, a realistic effective Lagrangian approach has been used that displays chiral symmetry, gauge invariance, and crossing symmetry, as well as a consistent treatment of the spin-3/2 interaction. The sensitivity to the elementary $\gamma N \to \pi N$ operator of the results has also been investigated.

Within our model, we have found that the inclusion of FSI effects is important for the helicity difference $d(\sigma^P - \sigma^A)/d\Omega$. πN rescattering appears to be less important compared to the NN rescattering in both neutral and charged channels. For the polarized total cross sections σ^P and σ^A as well as spin asymmetry $\sigma^P - \sigma^A$, we have found that the influence of FSI stems predominantly from NN rescattering, whereas πN rescattering is much smaller and appears only in σ^A close to threshold. In the neutral channel, we have observed that FSI effects lead to a strong reduction of the spin asymmetry and that σ^P is larger than σ^A. In charged channels, we have found that FSI effects appear mainly in σ^A near threshold. We have also found that $\sigma^P - \sigma^A$ starts out negative due to the E_{0+} multipole and has a strong positive contribution at higher energies due to the M_{1+} multipole. Regarding the results of E asymmetry, we have found qualitatively a similar behavior for all channels. We have also found that the influence of the FSI effects is strong, especially in the neutral channel at forward angles and low energies. We have also evaluated the contributions of separate channels to the GDH integral by explicit integration up to 350 MeV. A total value of the GDH integral of $I^{\rm GDH}_{IA+NN+\pi N}(350\ {\rm MeV}) = 41.29\ \mu$b has been computed after including FSI effects. A large positive contribution to the GDH integral came from the π^0-production channel, whereas the charged pion channels gave a negative but—in absolute value—smaller contribution to the GDH integral.

We have also studied the influence of the elementary operator in the polarized differential and total cross sections, E asymmetry, and GDH integral. The observables, for both the neutral and charged channels, are found to be very sensitive to the elementary operator. In many cases, the deviation among results obtained using different operators is very large. In view of these results as well as those presented in Ref. [1], we conclude that the process $d(\gamma,\pi)NN$ can serve as a filter for different elementary operators because their predictions provide very different values for observables.

The GDH integral is found to be an excellent observable to discriminate among different elementary pion production operators. We obtain quite different values for the GDH integral for the MAID and the ELA models, in spite of the fact that their predictions for the $\sigma^P - \sigma^A$ observable seem similar (see Fig. 8). Due to an important cancellation of the contributions below and above a photon energy of 260 MeV the pionic contribution to the GDH integral up to 350 MeV computed in this work gives 42 μb, what is relatively small compared to other contributions. The rest should be either coherent pion production or two-nucleon breakup [12].

Finally, we would like to point out that future improvements of the present model (in particular, its extension to higher energies) can be achieved including the next leading correction from the intermediate NN, NN^*, and $N\Delta$ interactions. Polarization observables in general constitute more stringent tests for theoretical models due to their sensitivity to small amplitudes. At this point, a much needed measurement on the deuteron spin asymmetries will certainly provide us with an important observable to test our knowledge of the pion photoproduction on the neutron process and, hence, to provide us with valuable information on the neutron spin asymmetry in an indirect way. An independent test within the framework of effective field theory will be also of great interest.

ACKNOWLEDGMENTS

One of us (E.M.D.) thanks A. Abdulnaby for keen interest to provide assistance with computing difficulties. C.F.-R. work has been partly developed under Spanish Government grant UAC2002-0009. C.F.-R. and E.M.G. acknowledge partial support from Ministerio de Educación y Ciencia (Spain) under contract FIS2005-00640. J.M.U. acknowledges partial support from Ministerio de Educación y Ciencia (Spain) under contracts BFM2003-04147-C02-01 and FPA2006-07393. E.M.G. and J.M.U. acknowledge partial support from UCM and Comunidad de Madrid under project number 910059 (Grupo de Física Nuclear).

[1] E. M. Darwish, C. Fernández-Ramírez, E. Moya de Guerra, and J. M. Udías, submitted (2007).

[2] M. I. Levchuk, A. Yu. Loginov, A. A. Sidorov, V. N. Stibunov, and M. Schumacher, Phys. Rev. C **74**, 014004 (2006).

[3] H. Arenhövel and A. Fix, Phys. Rev. C **72**, 064004 (2005); A. Fix and H. Arenhövel, Phys. Rev. C **72**, 064005 (2005); M. Tammam, A. Fix, and H. Arenhövel, Phys. Rev. C **74**, 044001 (2006).

[4] E. M. Darwish, H. Arenhövel, and M. Schwamb, Eur. Phys. J. A **16**, 111 (2003).

[5] B. Krusche and S. Schadmand, Prog. Part. Nucl. Phys. **51**, 399 (2003); V. Burkert and T.-S. H. Lee, Int. J. Mod. Phys. E **13**, 1035 (2004); D. Drechsel and L. Tiator, Annu. Rev. Nucl. Part. Sci. **54**, 69 (2004); H. Dutz *et al.*, Phys. Rev. Lett. **93**, 032003 (2004); K. Helbing, Prog. Part. Nucl. Phys. **57**, 405 (2006).

[6] C. A. Rovelli, M.Sc. thesis, University of Pavia, Italy (2002); O. Jahn, in *Proceedings of the 3rd International Symposium on the Gerasimov-Drell-Hearn Sum Rule and Its Extensions (GDH 2004), Norfolk, Virginia, June 1–5* (2004); A. Braghieri, in *Proceedings of the 10th International Conference on the Structure of Baryons (BARYONS 2004), Ecole Polytechnique, Polaiseau, France, 25–29 October* (2004); A. Thomas and M. Martínez Fabregate, in *Proceedings of the Symposium of Twenty Years of Physics at the Mainz Microtron (MAMI), J. Gutenberg-Universität, Mainz, Germany, 19–22 October* (2005), http://wwwa1.kph.uni-mainz.de/Symposium/talks/; T. Rostomyan, Ph.D. dissertation, Gent University (2005); H.-J. Arends, in *Proceedings of the 9th Conference on the Intersections of Particle and Nuclear Physics (CIPNP 2006), Westin Rio Mar Beach, Puerto Rico, 30 May–03 June* (2006); T. Rostomyan and P. Pedroni, in *23rd Students' Workshop on Electromagnetic Interactions, Bosen (Saar), Germany, 3–8 September* (2006); A. Thomas, Eur. Phys. J. A **28**, Suppl. 1, 161 (2006); M. Martínez Fabregate, Ph.D. dissertation, J. Gutenberg-Universität, Mainz, Germany (2007); P. Pedroni (private communication); T. Rostomyan, Nucl. Phys. **A755**, 451c (2005); J. Ahrens *et al.*, Phys. Rev. C **74**, 045204 (2006).

[7] J. Ahrens *et al.*, Phys. Rev. Lett. **97**, 202303 (2006); Phys. Rev. Lett. **98**, 039901(E) (2007) .

[8] LEGS@BNL Collaboration, A. M. Sandorfi *et al.*, http://www.legs.bnl.gov; A. M. Sandorfi (private communication).

[9] S. B. Gerasimov, Yad. Fiz. **2**, 598 (1965) [Sov. J. Nucl. Phys. **2**, 430 (1966)]; S. D. Drell and A. C. Hearn, Phys. Rev. Lett. **16**, 908 (1966).

[10] E. M. Darwish, H. Arenhövel, and M. Schwamb, Eur. Phys. J. A **17**, 513 (2003).

[11] E. M. Darwish, Nucl. Phys. **A748**, 596 (2005).

[12] H. Arenhövel, A. Fix, and M. Schwamb, Phys. Rev. Lett. **93**, 202301 (2004); H. Arenhövel, A. Fix, and M. Schwamb, in *Proceedings of the 3rd International Symposium on the Gerasimov-Drell-Hearn Sum Rule and its Extensions (GDH 2004), Norfolk, Virginia, 1–5 June* (2004), edited by S. Kuhn and J.-P. Cheng (World Scientific, Singapore, 2005), pp. 294; M. Schwamb, Eur. Phys. J. A **28**, Suppl. 1, 39 (2006).

[13] R. Schmidt, H. Arenhövel, and P. Wilhelm, Z. Phys. A **355**, 421 (1996).

[14] D. Drechsel, O. Hanstein, S. Kamalov, and L. Tiator, Nucl. Phys. **A645**, 145 (1999); D. Drechsel, S. S. Kamalov, and L. Tiator, Phys. Rev. D **63**, 114010 (2001); MAID Program, http://www.kph.uni-mainz.de/MAID/maid2003/

[15] C. Fernández-Ramírez, E. Moya de Guerra, and J. M. Udías, Ann. Phys. (NY) **321**, 1408 (2006).
[16] C. Fernández-Ramírez, Ph.D. dissertation, Universidad Complutense de Madrid, Spain (2006), http://nuclear.fis.ucm.es/research/thesis/cesar_tesis.pdf.
[17] M. Lacombe, B. Loiseau, J. M. Richard, R. Vinh Mau, J. Cônté, P. Pirès, and R. de Tourreil, Phys. Rev. C **21**, 861 (1980).
[18] J. Haidenbauer and W. Plessas, Phys. Rev. C **30**, 1822 (1984); **32**, 1424 (1985).
[19] S. Nozawa, B. Blankleider, and T.-S. H. Lee, Nucl. Phys. **A513**, 459 (1990).
[20] C. Fernández-Ramírez, E. Moya de Guerra, and J. M. Udías, Phys. Rev. C **73**, 042201(R) (2006); Eur. Phys. J. A **31**, 572 (2007).
[21] Review of Particle Physics, W.-M. Yao *et al.*, J. Phys. G **33**, 1 (2006).
[22] C. Fernández-Ramírez, E. Moya de Guerra, and J. M. Udías, Phys. Lett. **B651**, 369 (2007).
[23] V. Pascalutsa, Phys. Rev. D **58**, 096002 (1998); V. Pascalutsa and R. Timmermans, Phys. Rev. C **60**, 042201(R) (1999).
[24] R. A. Arndt, W. J. Briscoe, I. I. Strakovsky, and R. L. Workman, Phys. Rev. C **66**, 055213 (2002), SAID database, http://gwdac.phys.gwu.edu.
[25] D. G. Ireland, S. Janssen, and J. Ryckebusch, Nucl. Phys. **A740**, 147 (2004).